VIBRATION MODES OF LOGS MEASURED BY TV HOLOGRAPHY

Sondre Skatter

Norwegian Forest Research Institute
Høgskolevn. 12
N-1432 Aas
Norway

Astrid Aksnes Dyrseth

Applied Optics Group, Physics Department
Norwegian University of Science and Technology
N-7034 Trondheim
Norway

(Received October 1996)

ABSTRACT

Resonant vibrations of softwood logs were examined using TV holography. This technique allows a resonance to be detected in real time when the frequency is varied. Time-averaged measurements can be taken to map the spatial vibration pattern of the object both at resonance and at an arbitrary frequency. The resonant frequency of an identified vibration mode is used to calculate certain material parameters. Here, the longitudinal modulus of elasticity is determined from bending modes using Timoshenko's beam theory, and one of the shear moduli is determined from torsion modes. Additionally, the vibration patterns may reflect inhomogeneities within the logs. A feasibility study was made on the possibilities of detecting knots from the vibration patterns of a particular mode of vibration. It was concluded that this is not, in general, possible.

Keywords: Vibration analysis, TV holography, logs, bending, torsion.

INTRODUCTION

The vibrational behavior of logs represents a great potential in assessing information about mechanical characteristics of a log. Different types—or modes—of resonant vibration are associated with different material parameters, which can be estimated using a theoretical model when an experimental value of the resonant frequency is known. Moreover, the vibration pattern of a single mode might reflect structural inhomogeneities within the log that are invisible on the surface.

Possible applications of vibration analysis applied to logs are:

- Assessment of elastic constants such as the longitudinal Young's modulus (MOE) and one of the shear moduli that can be used in quality sorting of logs prior to processing. For the sawmilling industry, this means that the quality of the lumber to be sawn from a log can be predicted by the MOE of the log. Galligan et al. (1967) proposed that longitudinal vibrations could be used to determine the log's MOE, while Ross et al. (1996) recently suggested the use of longitudinal stress waves for the same purpose.
- Detection of structural inhomogeneities such as knots, checks, and decay. If these defects are localized prior to sawing, an optimized sawing pattern can be chosen, i.e., a sawing pattern that maximizes the value of the lumber. Several technologies have previously been proposed for this purpose: tomographic techniques such as X-ray (or gamma) computed tomography (CT) (Taylor et al. 1984; Birkeland and Holøyen 1987) and nuclear magnetic resonance (NMR) (Wang and Chang 1986) have proven to locate knots with a spatial resolution far beyond the demands. However, this type of scanning is still too slow to be operated in an on-line sawmill system. Scanning systems involving ultrasonics have also been

proposed and studied (Han 1991). All these techniques involve time-consuming scanning, which results in an enormous amount of data needed to reconstruct a physical parameter, such as density, into discrete volume elements.

- A tool for tree scientists who want to understand the mechanics of standing trees. A tree might be put into resonant vibrations by external forces e.g., wind load, or be deformed in a similar pattern statically. Either way, the laboratory vibration measurements reveal the susceptibility of trees to forces that may cause failure in bending or torsion.

In this study, elastic parameters of a sample of pine logs were determined from measurements of the bending and torsion vibrations. Furthermore, we investigated if TV holography can be used to detect knots by studying the knots' influence on the resonant vibration patterns. A pilot study involving a single specimen, a spruce log, indicated the existence of a class of modes, transverse modes, which enabled branch whorls to be localized in a special manner.

THEORETICAL DESCRIPTION

Resonant vibrations

Natural vibration of wooden objects reflects the elastic property of wood. A set of vibration modes, or eigenmodes, constitute the dynamic nature of an elastic object. Each eigenmode is characterized by its modal parameters, which are the resonant frequency, the damping factor, and the mode shape, or vibration pattern (Skatter 1996). The mode shape is the spatial deflection pattern of the vibrating object surface. Since this deflection pattern is time-varying, it must be described by two numbers—the amplitude, defined as the maximum deflection, and the relative phase of vibration. At resonance, the vibration pattern is a standing wave and the phase can take only two values separated by 180°. At nodal lines the amplitude is zero, and when crossing this line there is a phase shift of 180°.

A vibration mode can be excited in two ways: either by an initial disturbance that leaves the object vibrating freely at a resonant frequency, or by a periodic force acting upon the object with a periodicity at or near a resonant frequency. The latter is preferable when the aim is to image the vibration modes. When the frequency of the periodic force is arbitrary, i.e., not coincidental with a resonant frequency, the vibration pattern is not a standing wave but a complex picture of traveling waves.

To predict material parameters on the basis of vibration analysis, a theoretical description of the vibration is required. By setting a theoretical expression of the resonant frequency equal to the measured frequency of the same mode, the desired material parameter can be resolved from the equation and determined.

Classes of vibration modes

In the experimental setup to be described, only transverse components of displacement are detectable, and longitudinal motion is therefore not observed.

Bending.—Bending is a vibration mode that exists in practically every oblong elastic object (also referred to as flexural vibration). If the cross section is uniform and the length-to-depth ratio is sufficiently large (~20), the object will undergo pure bending where the only non-zero stress component is the normal longitudinal component, σ_L. Euler beam theory applies (Hearmon 1966) under these conditions. When the log is free at both ends (i.e., there are no external forces from supports), the modulus of elasticity, E_{EUL}, can be expressed in terms of the resonant frequency, f_{B-n}, as in Eq. (1).

$$E_{EUL} = \frac{4A\rho L^4 f_{B-n}^2}{\pi^2 \gamma_n^2 I} = \frac{16\rho L^4 f_{B-n}^2}{\pi^2 \gamma_n^2 R^2}, \quad (1)$$

where:

n = mode number
I = moment of inertia = $\pi R^4/4$ for cylinders (R = cylinder radius)
A = cross section area = πR^2 for cylinders
ρ = mass density
L = length of the object.

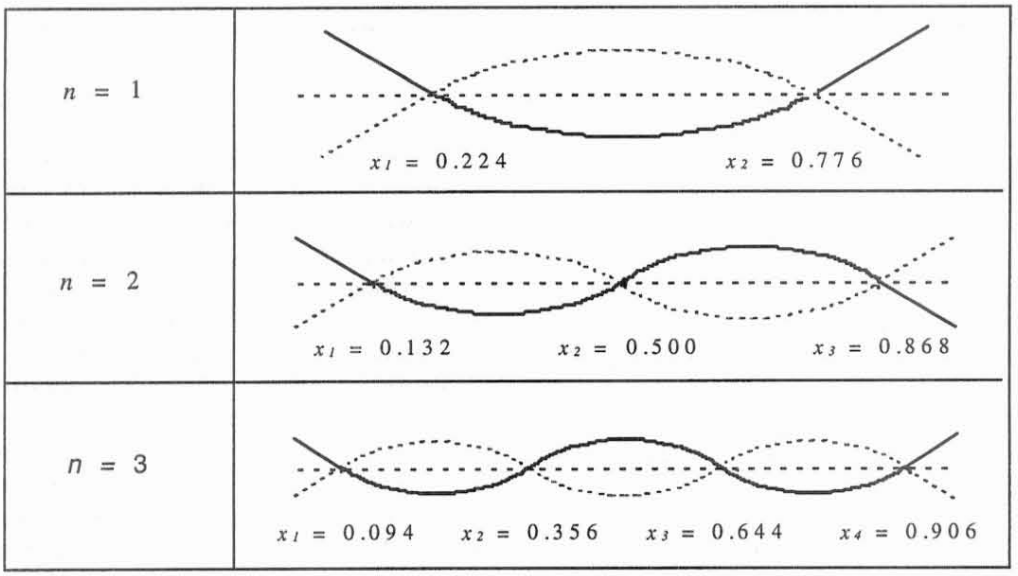

FIG. 1. Mode shapes of the three first bending modes with the free-free ends support conditions. The nodal points are marked.

$\gamma_1 = 2.267$, $\gamma_2 = 6.249$, $\gamma_n \cong (n + \frac{1}{2})^2$ for $n > 2$

The corresponding mode shapes are sketched roughly in Fig. 1. When the resonant frequency of a bending mode is known from experiments, the modulus of elasticity can be calculated using Eq. (1). However, when the length-to-depth ratio is less than 15 as in this case, shear deformation and rotary inertia will influence the frequency and this must be accounted for by altering the frequency equation. Timoshenko beam theory (Hearmon 1966) takes into account both shear and rotary inertia, and one particular solution to this equation was obtained by Goens (1931). This solution is given for the free-free ends support condition in Eq. (2):

$$E = E_{EUL} T_n$$

$$T_n = 1 + \frac{R^2}{4L^2}\left(F_1(n) + \frac{E}{\beta G} F_2(n)\right) - \frac{\pi^2 \rho R^2 f_{B-n}^2}{\beta G}, \quad (2)$$

where the numerical factors $F_1(n)$ and $F_2(n)$ are listed in Hearmon (1966). G denotes an effective shear modulus, which is a weighted average of G_{LR} and G_{LT}, while β is an unknown form factor. Since neither β nor the weighting factors in G are known, we will consider the factor $\eta = 1/\beta G$ as the second unknown. The resonant frequency of at least two bending modes must be measured to determine E and η. In the experiments to be described later in this paper, 4 (5) bending modes are measured for each log, which means that 6 (10) combinations of modes exist yielding a value of E and η. Another possibility is to find the values of η and E that minimize the sum of the square errors of Eq. (2), $\Sigma_n(E - E_{EUL,n}T_n)^2$. Since the 4 (5) equations are not completely consistent, the latter is preferred for our calculations.

Torsion.—Torsional vibration modes have a similar longitudinal behavior to that of the bending modes. The first mode has one nodal line in the middle of the log, while the second one has two nodal lines, etc. For logs, if we assume circular cross sections, only one shear modulus is associated with the torsion modes, namely G_{LT}. According to Euler-St. Venant theory, this modulus may be expressed by the resonant frequencies as:

$$G_{LT} = \left(\frac{2Lf_{T-n}}{n}\right)^2 \rho \quad (3)$$

One should be aware that Eq. (3) must be modified if the density is not uniform over the cross section, e.g., due to heartwood/sapwood. In this case, ρ should be replaced by:

$$\rho = \rho_{sap} - (\rho_{sap} - \rho_{heart})\left(\frac{R_{heart/sap}}{R}\right)^4 \quad (4)$$

where $R_{heart/sap}$ is the radius at the heartwood/sapwood boundary.

Transverse modes.—As previously mentioned, longitudinal motion is not detectable with the experimental setup described. However, according to the theory of elasticity, an applied uniaxial force will not only cause normal strain in the force direction, but also strains in the transverse directions, the amount given by the Poisson numbers. As a consequence, the axial modes may be detectable due to the passive transverse strains. It is to be expected that modes exist where the primary deformation is in the transverse strain components. Since longitudinal and transverse normal strains in general are coupled, it is difficult to class a mode as purely transverse normal or longitudinal.

MEASURING SINUSOIDAL VIBRATIONS BY TV HOLOGRAPHY

TV holography is a nondestructive technique used for full-field vibration and deformation analysis. A video camera is used as the recording device allowing measurements in near real time. For a more detailed description of the technique, we refer to the literature (Løkberg 1980; Løkberg and Slettemoen 1987; Jones and Wykes 1989).

The experimental setup used for the vibration analysis of logs is shown schematically in Fig. 2. Coherent light from an argon laser is split into two branches, the reference branch and the object branch. The laser beam in the object branch is passed through a speckle averaging mechanism (SAM) before it is expanded by a lens to illuminate the sinusoidally vibrating log. The SAM is used to improve the quality of the recording by altering the object illumination in small steps, thus averaging the scattered light from the log. The scattered object light is combined with a reference beam where the phase is sinusoidally varying at the same frequency as the object (log). The resulting interference pattern is time-average recorded by the video camera. The video signal is then reconstructed electronically in the signal processing unit allowing the image of the object overlaid with interference fringes (the vibration pattern) to be seen on the monitor in real time and interference fringes superimposed on the image of the object can be seen on the monitor. By shifting the phase of the reference beam with the phase modulator and using phase-stepping algorithms, the phase and amplitude can be determined quantitatively (Løkberg 1984; Ellingsrud and Rosvold 1992). Resonant vibrations can be manually detected by varying the frequency and observing the vibration pattern on the video monitor. When a resonance is detected, a phase-stepped measurement can be made to reconstruct the vibration phase and amplitude (Skatter 1996).

MATERIALS AND METHODS

Two series of experiments are described. The first trial included only a single specimen, a short spruce log. The resonant vibrations found on this log led to the proposal of a hypothesis which, if true, would allow the detection of branch whorls on the basis of a special class of vibrations modes.

The second series consisted of four pine logs where one log was completely free from knots in the interior. The dimensions and densities of the logs are specified in Table 1. The aforementioned elastic parameters were calculated for these samples.

General description of the experimental setup

The logs were barked and painted with a retroreflective paint in order to increase the reflectivity of the log surface. A mirror was placed at an angle behind the log to image part

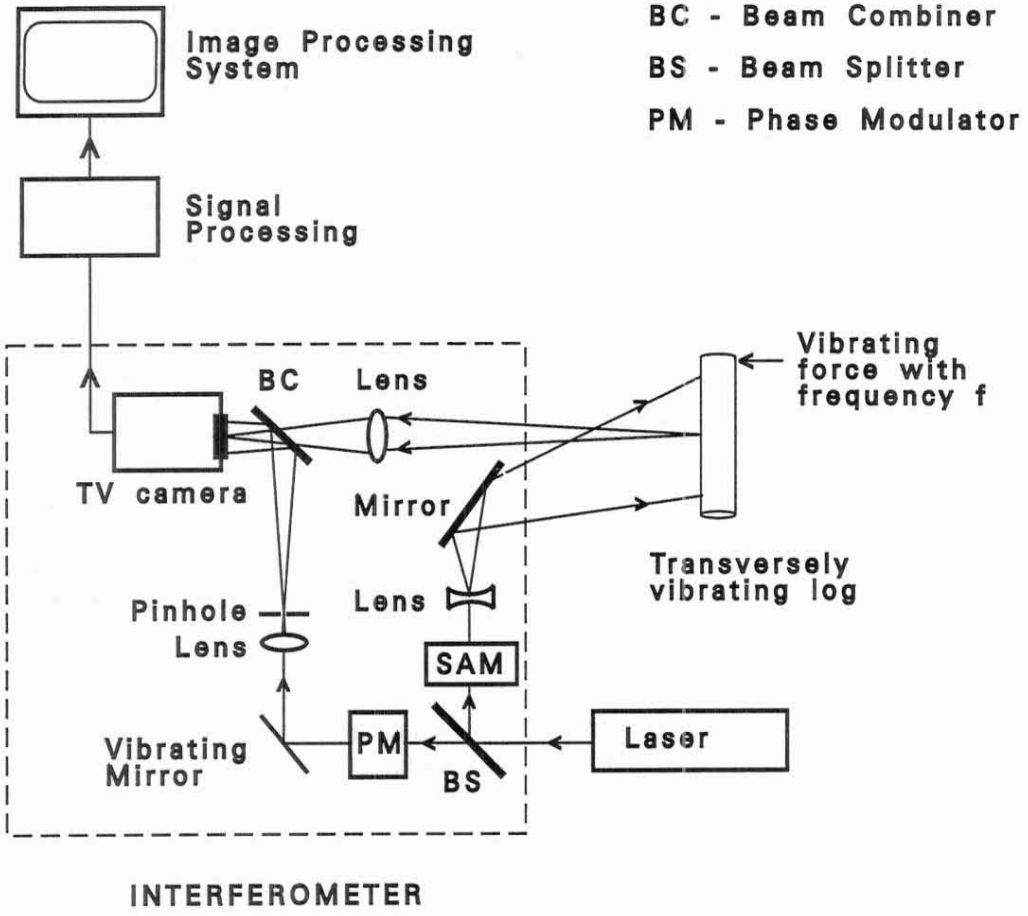

FIG. 2. Principal setup of the applied TV holography system.

of the top and back side of the log. Monitoring both the front and back side of the log is a key to understanding the vibration mode. The interferometer, a RETRA 1000 (from Conspec A/S, Trondheim), was supplied with light from an argon laser via an optical fiber.

When bending modes were excited, the log was supported on foam rubber placed underneath the ends to simulate free-free ends condition. The shaker was placed against the log with a horizontal radial direction of force as illustrated in Fig. 3a. To excite a bending mode, the excitation point cannot coincide with a nodal line. When exciting torsional

TABLE 1. *Summary of the characteristics of the pine logs. The density is the average of two determinations: one is the total mass divided by an estimate of the volume; the other uses values achieved from CT-scanning of the logs. The uncertainty is the standard deviation of the two values.*

Log	Knots	Length (m)	Diameter top/butt (mm)	Average density (kg/m^3)
1a	No knots	2.00	151/158	1,015 ± 30
2b	Regular branch whorls	2.00	145/153	1,015 ± 15
1b	Regular branch whorls	1.43	164/180	1,085 ± 30
2c	Grown-over knots	1.43	159/178	940 ± 15

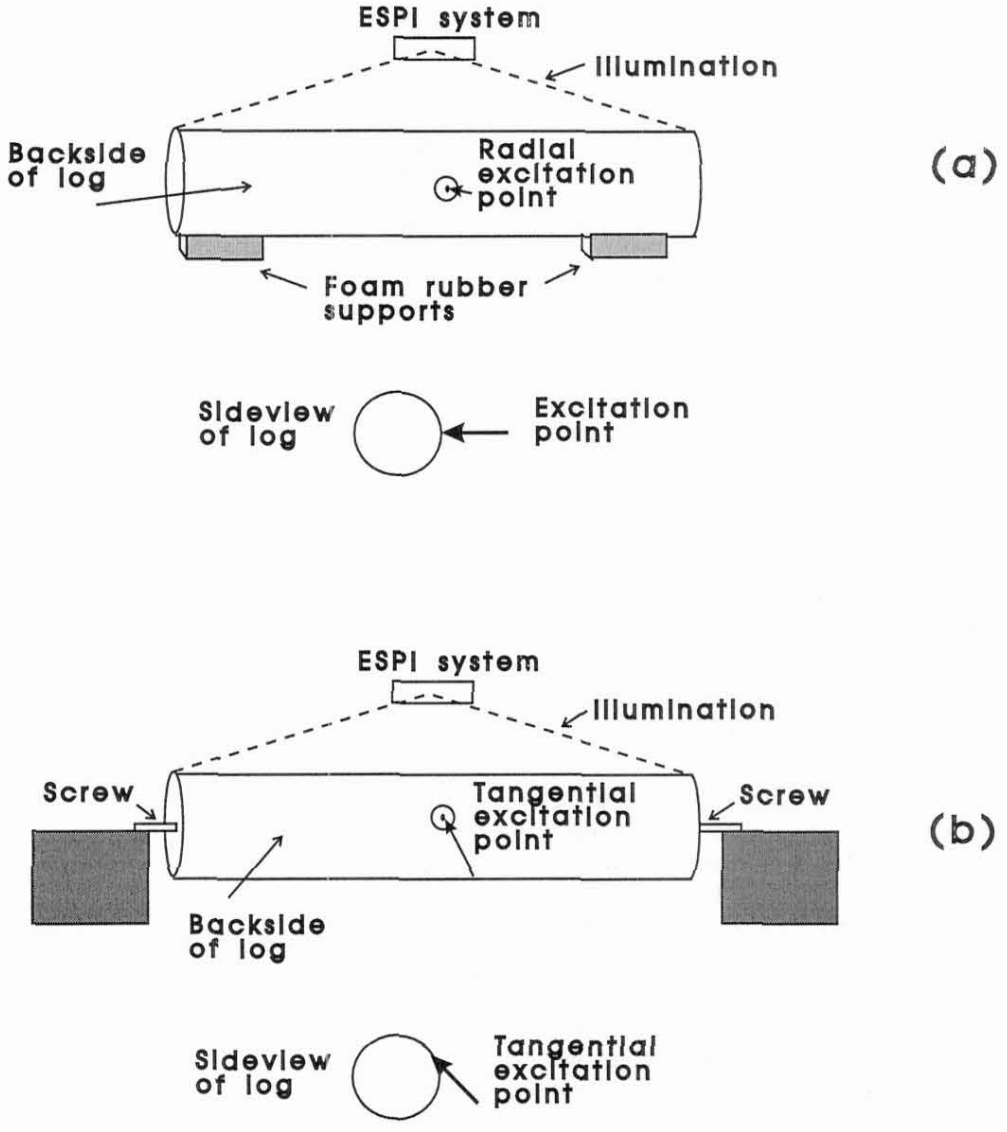

FIG. 3. Methods of support to ensure free-free ends condition for a) bending modes and b) torsional modes.

modes, the log was hung up on screws which were screwed into the pith as shown in Fig. 3b. This method of support proved to be very good because the cylinder center is fixed, and tangential motion is allowed elsewhere. The shaker was placed against the log with a tangential component of force. When searching for the transverse modes introduced previously, the log was hung up on screws as with torsion modes, and the shaker was placed with a horizontal radial direction as for the bending modes.

The first results and the formulation of the hypothesis

The spruce log was 79.5 cm long, 20 cm in diameter on average, and it had two branch whorls. The longitudinal positions of the branch whorls are shown in Fig. 4.

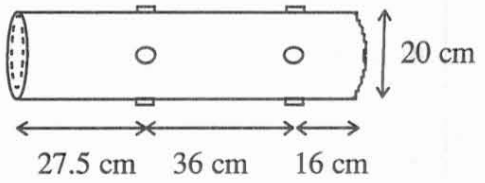

FIG. 4. Dimensions of spruce log indicating the longitudinal positions of the branch whorls.

Bending modes were found at the frequencies 790 Hz (first), 1,572 Hz (second), and 1,940 Hz (third). The log was cut slightly shorter when the second bending mode was determined. Theoretically predicted nodal lines (Fig. 1) were compared with the phase image of the mode identified as the first bending mode (Fig. 5). There was good agreement except to the right in the image where a small part of the log had not been imaged. The front and the back side of the log (seen in the mirror) had opposite phases, which means that they move in the same directions in a Cartesian coordinate system.

More interesting is the other class of vibration modes observed on the spruce log. For the bending modes, the center of mass moves transversely; but in this other type of transverse vibration, the center of mass seems to be at rest. Here, the origin of the transverse vibrations is deformation of the cross-sectional shape. In bending, the cross-sectional shape is deformed only as a secondary effect due to passive strains caused by the longitudinal stress. The results indicated that the cross-sectional displacement for the different modes had the angular dependency of Fourier series components Eq. (5):

$$\left.\begin{aligned} u(r, \theta) &= f(r)\cos(n\theta) \\ v(r, \theta) &= g(r)\sin(n\theta) \end{aligned}\right\}, \qquad n = 1, 2, 3, \ldots, \tag{5}$$

where r is the radial position, θ the angular position, and u and v are the radial and tangential displacements, respectively. The transverse displacement patterns for n = 0, 2, 3, 4 are plotted in Fig. 6. Such a displacement field can, according to Mirsky (1964), be expected

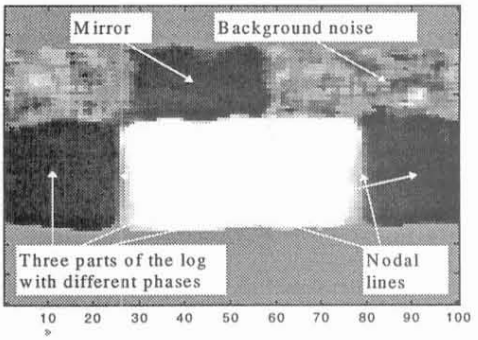

FIG. 5. Phase image of the first bending mode occurring at 790 Hz. The predicted nodal lines are at 0.224 and 0.776 (when the length of the log equals 1). The front and the back side of the log (seen in the mirror) had opposite phases, which means that they move in the same Cartesian directions.

if the material is transversely isotropic, i.e., the elastic properties are equal in the radial and tangential directions. In general, this is not the case for wood. It should be noted that the experimental setup used has its weaknesses when measuring displacement patterns described by Eq. (5). The displacement direction is in the radial direction, while the TV holography setup senses only components of displacement in the illumination direction. Consequently, the amplitude of displacement is correctly determined only where the radial direction coincides with the horizontal direction

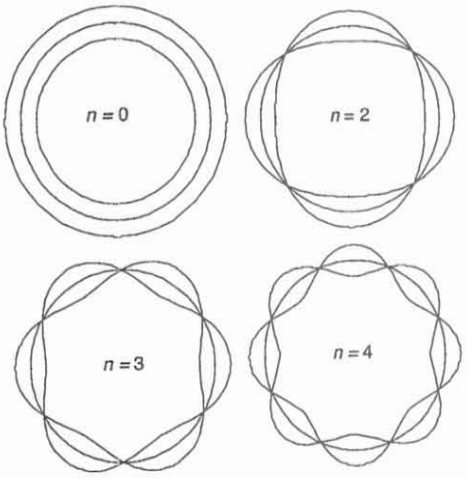

FIG. 6. Mode shapes of the transverse modes of form (4).

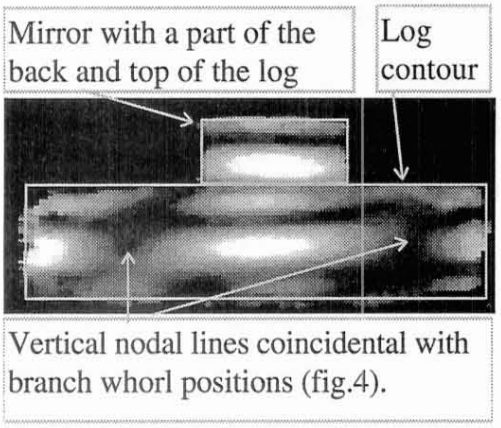

FIG. 7. Amplitude image of transverse mode at 1,845 Hz (n = 3). High intensity denotes high amplitude. The vertical nodal lines are black areas, i.e., zero amplitude where the corresponding phase images have a shift of 180°.

at the front. At the very top and bottom of the log, the displacement direction is vertical and cannot be detected. An angularly dependent weight factor should be multiplied with the amplitude while the phase of vibration is correctly determined. This is important to keep in mind when interpreting the vibration images.

The displacement field of the transverse modes seemed to have a longitudinal dependence on the position of knots. Figures 7 and 8 show amplitude images of vibration modes occurring at 1,845 and 2,950 Hz. Both figures show that vertical nodal lines are located at the same position as the branch whorls (ref. Fig. 4). By counting the peripheral phase shifts on the visible front side, the modes in Figs. 7 and 8 can be identified as the n = 3 mode and the n = 5 mode, respectively. The mode number is the number of waves around the circumference of the log cross section (see Fig. 6).

The results presented above lead to the proposal of the hypothesis:

- Vibration modes with the circumferential displacement pattern described by Eq. (5) exist in logs
- Knots counteract the radial displacement, and transverse nodal lines will therefore occur at the longitudinal positions of the branch whorls.

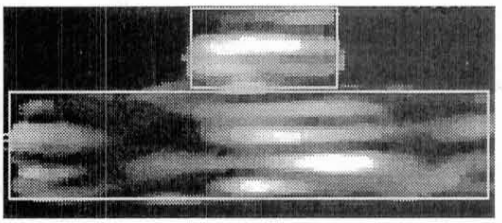

FIG. 8. Amplitude image of transverse mode at 2,950 Hz (n = 5).

The specimens for the second experiment were chosen in order to confirm or reject this hypothesis.

The second experiment—testing of the hypothesis

A new material was chosen to test the hypothesis proposed above. Scots pine was chosen because of greater regularity with respect to branch whorls, i.e., there are no knots between the branch whorls as in spruce. Log 1a was completely knot-free. The knots had been removed immediately after the budding had taken place (Russian pruning). A control log was chosen with approximately the same dimensions (2b) as the knot-free log but with regular branch whorls. The two last logs were similar regarding dimensions, but the knots in log 1b reached the surface, while the other log (2c) had only grown-over knots except for a few small encased knots. The density values used in the later calculations are the average values of two density determinations. The first of these was based on the total mass and an estimate of the volume, while in the other method the density was determined from CT-scanning of the logs. In the latter, an average over the log cross section was used. The properties of the specimens are summarized in Table 1.

RESULTS

Transverse modes

Transverse modes were not observed on the pine logs. Longitudinally traveling waves with

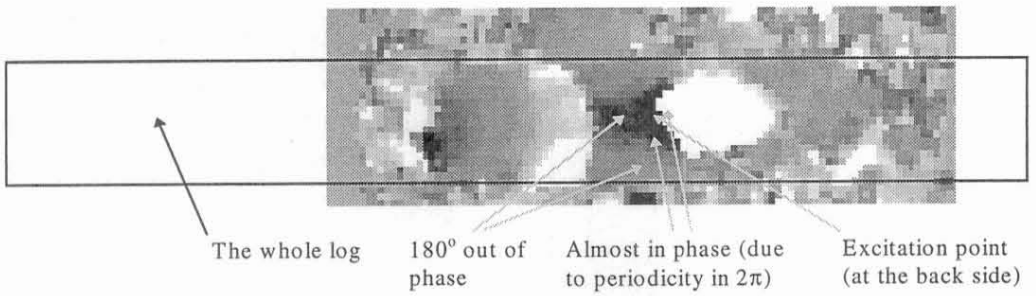

FIG. 9. Phase plot of vibration pattern on knot-free log at 2,138 Hz. In the vicinity of the excitation point, the mode has an n = 3 shape while it turns to n = 0 after propagation towards left.

an initial circumferential shape as specified by Eq. (5) were observed, but no resonant vibration of this kind was found. The phase image of one of these traveling waves measured on the knot-free log (1a) is shown in Fig. 9. This vibration pattern was recorded while the vibrating force was working at the middle of the visible part of the log. The phase does not take only two values anymore; the continuous change of phase to the left is describing a propagating wave. Animation shows that waves propagate both to the left and to the right from the excitation point. When the excitation point was moved, waves propagated from the new position similarly. It is interesting that, in the vicinity of the excitation, the deflection pattern is that of Fig. 6 with n = 3. At a certain point, as the wave propagates longitudinally, the circumferential shape alters to n = 0 (or n = 1).

Similar vibration patterns were recorded on specimen 2b. Transverse modes were not observed here either, but interesting nonresonant vibration patterns were recorded. Vibration patterns corresponding to the one in Fig. 8 were recorded with n = 2, 3, 4. Whether the branch whorls played an important role here is hard to tell because the vibration patterns are very dependent on the excitation point in cases of nonresonant vibrations.

The hypothesis must therefore in general be rejected. Special circumstances around the first specimen, the spruce log, may explain why whorls were identified. Possible explanations are:

- The anisotropy of pine is more pronounced than that of spruce, that is, G_{LT} is very different from G_{LR} and E_R different from E_T (Kollmann and Côté 1968) and/or
- There are two equations that have to be satisfied at resonance—one involving the radius and the number of circumferential waves (n) and one involving the longitudinal nodal distance (distance between branch whorls). Only one parameter is free, namely the frequency. By coincidence, the combination of radius and internodal distance fit the spruce log, while this was not the case with the pine logs.

TABLE 2. *The resonant frequencies of the bending modes. The MOE (E) is determined by minimizing the sum of the square error of the 4 (5) equations in Eq. (2).*

Log	1st. (Hz)	2nd. (Hz)	3rd. (Hz)	4th. (Hz)	5th. (Hz)	E (GPa)	$E/\beta G$
1a	120	286	492	708	920	13.7	23.3
2b	116	273	460	652	852	13.9	29.6
1b	239	550	880	1,206	—	13.8	17.9
2c	250	556	871	1,194	—	14.0	23.0

Bending modes

Bending modes were observed for all the specimens. All the results can be seen in Table 2 along with the calculated elastic parameters. These parameters are only apparent elastic parameters, i.e., they are global values for each log. The actual moduli vary within each log. E and η are determined by minimizing the sum of the square error of Eq. (2) for all the

TABLE 3. *The observed torsion modes. The shear modulus G_{LT} is determined by use of Eq. (3) with an approximate expression for ρ in Eq. (4) derived by measuring the density of heartwood and sapwood and the radius of the heartwood/sapwood limit in a CT scanner. The numbers in parentheses are the values determined from modes 1, 2, and 3 respectively.*

Log	1st. (Hz)	2nd. (Hz)	3rd. (Hz)	G_{LT} (GPa)
2b	190	381	569	0.62 (0.623, 0.626, 0.620)
1a (cut to 0.67 m)	626	—	—	0.76

4 (5) modes for each log. The calculated MOEs are almost equal for all the logs, at least not significantly different because the uncertainties in the densities (Table 1) are in the same order of magnitude as the difference between the MOEs. The effective shear modulus G, when assuming both β and E constant, has a much larger variation, even though there is no obvious pattern of this variation. Chui (1991) states from bending tests that on average the shear modulus is higher for knotty specimens than for clearwood.

The values of E are somewhat high compared to what should be expected from literature (Kollmann and Côté 1968). According to literature, dynamic MOEs are 8–10% higher than the static values due to the viscoelastic nature of wood. The values determined here are still, however, much higher than would be expected. Spot tests in terms of a few small clear specimens were taken from three of the logs; 2b, 1b, and 2c. Static MOE was measured in accordance with ISO 3349 (1975). These tests showed that the MOE varied very much within each log; for 1b the values ranged between 7.5–10.2 GPa, for 2b between 7.7–11.7 GPa, and for 2c between 8.1 to 10.4 GPa. It is difficult to calculate an effective MOE for the log, but it is interesting to note that the local variations of MOE are organized in a way that makes the effective MOE of the trunk high compared to the local values. This may be a new example of optimized growth.

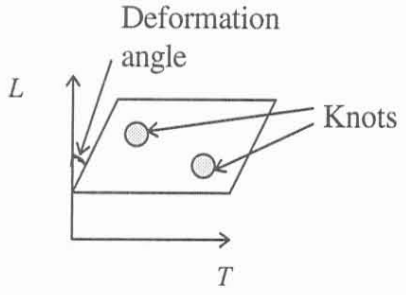

FIG. 10. The intersection of knots and the LT-plane.

Torsion modes

Torsion modes were measured on only two of the specimens. They were very easy to find when the support condition and the imposed force were as specified above. Torsion modes were measured on log 2b and log 1a (log 1a after being cut to one third of its original length), and the results can be seen in Table 3. We see that the calculated value of G_{LT} for 2b is the same for all the three modes. In contradiction to bending, this is a pure mode, i.e., the torsion deformation does not couple to other deformation modes.

Log 2b has 18% lower shear modulus than the knot-free 1a. In the deformation plane, LT, all the knots intersect perpendicularly (Fig. 10), and this may cause the decrease in the shear modulus.

Just as with the bending deformation, torsion is likely to occur in living trees due to asymmetrical crowns, and the vibrational behavior might be related to failure of standing trees.

CONCLUSIONS

The results do not show that interior defects in logs, such as knots, in general can be detected from resonant vibrations. The pine logs did not behave as assumed after the pilot study on a spruce log. A theoretical analytical approach to these wave phenomena might clarify the picture.

The MOE was determined by using Timoshenko beam theory and was for all the pine logs about 14 GPa. Spot tests of small clear specimens from the logs resulted in local values of static MOE between 7.5 and 11.7 GPa, so even when the normal difference between static and dynamic MOE is taken into account, the global value of MOE is high. The shear modulus varied greatly between the logs.

The shear modulus G_{LT} was determined from the torsion modes, and the results indicate that knots decrease the value of G_{LT}.

ACKNOWLEDGMENTS

This work was supported by the Norwegian Research Council.

REFERENCES

BIRKELAND, R., AND S. HOLØYEN. 1987. Industrial methods for internal scanning of log defects: A progress report on an ongoing project in Norway. *In* Proc. 2nd International Conference on Scanning Technology in Sawmilling. Miller-Freeman Publications, San Francisco, CA.

CHUI, Y. H. 1991. Simultaneous evaluation of bending and shear moduli of wood and the influence of knots on these parameters. Wood Sci. Technol. 25:125–134.

ELLINGSRUD, S., AND G. O. ROSVOLD. 1992. Analysis of data based TV holography system used to measure small vibration amplitudes. J. Opt. Soc. Am. 9(2):237–251.

GALLIGAN, W. L., R. F. PELLERIN, AND M. T. LENTZ. 1967. A feasibility study: Longitudinal vibration of logs for prediction of lumber quality. Internal Rep. 4, Wood Technology Section, Engineering Research Division, Washington State University, Pullman, WA.

GOENS, E. 1931. Determination of Young's modulus from flexural vibrations (in German). Annalen der Physik 11(6):649–678.

HAN, W. 1991. An intelligent ultrasonic system for log scanning. Ph.D. thesis, Norw. Inst. of Technol., Trondheim, Norway.

HEARMON, R. F. S. 1966. Vibration testing of wood. Forest Prod. J. 16(8):29–39.

ISO STANDARD 3349. 1975. Wood—Determination of modulus of elasticity in static bending, Ed.1, 3p.(B), TC 55, @ International Organization for Standardization, Switzerland.

JONES, R., AND C. WYKES. 1989. Pages 165–196 *in* P. L. Knight, W. J. Firth, and S. D. Smith, FRS, eds. Holographic and speckle pattern interferometry. Cambridge Univ. Press, London, UK.

KOLLMANN, F. F. P., AND W. A. CÔTÉ. 1968. Principles of wood science and technology. Springer Verlag. Pp. 294–296.

LØKBERG, O. J. 1980. Electronic speckle pattern interferometry. Phys. Technol. 11:16–22.

———. 1984. ESPI—The ultimate holographic tool for vibration analysis. J. Acoust. Soc. Am. 75(6):1783–1791.

———, AND G. A. SLETTEMOEN. 1987. Basic electronic speckle pattern interferometry. Pages 455–504 *in* R. R. Shannon and J. Wyant, eds. Applied optics and optical engineering. 10, Academic Press, New York, NY.

MIRSKY, I. 1964. Wave propagation in transversely isotropic circular cylinders Part I: Theory. J. Acoust. Soc. Am. 36:41–51.

ROSS, R. J., D. W. GREEN, K. A. MCDONALD, AND K. C. SCHAD. 1996. NDE of logs with longitudinal stress waves. Pages 117–121 *in* J. L. Sandoz, ed. 10th International Symposium on Nondestructive Testing of Wood. EPFL, Lausanne, Switzerland.

SKATTER, S. 1996. TV holography as a possible tool for measuring transverse vibration of logs—A pilot study. Wood Fiber Sci. 28(3):278–285.

TAYLOR, F. W., F. G. WAGNER, C. W. MCMILLIN, I. L. MORGAN, AND F. F. HOPKINS. 1984. Locating knots by industrial tomography—A feasibility study. Forest Prod. J. 34:42–46.

WANG, P. C., AND S. J. CHANG. 1986. Nuclear magnetic resonance imaging of wood. Wood Fiber Sci. 18:308–314.